UNIVERSITAT DE BARCELONA

FACULTAT DE FÍSICA

Màster en Biofísica

Mechanochemical alterations of lung cells during fibrogenesis

Treball final del Màster en Biofísica 2008/09:
Irina Pavelescu

Tutor:Dr. Jordi Alcaraz
Unitat de Biofisica i Bioengineria, Facultat de Medicina, Universitat de Barcelona

Contents

Abstract

Idiopath pulmonary fibrosis (IPF) is a usually fatal disease associated with hardening of the lung tissue, epithelial injury and abnormal wound healing. Myofibroblasts are cells with smooth muscle like features and are believed to promote abnormal extracellular matrix (ECM) deposition, perpetuated scarring and loss of tissue function during fibrosis. These cells seem to arise either from epithelial cells via transforming growth factor (TGFβ1) induced epithelial to mesenchymal transition (EMT) or from the activation of resident fibroblasts through TGFβ1 mediated fibroblast to myofibroblast transition (FMT). We treated with TGFβ1 three human lung epithelial cell lines (H441, A549, H1975) and primary lung fibroblasts from three healthy patients and from three IPF patients. We used immunofluorescence techniques in order to quantify the expression of various cytoskeletal proteins (F-actin, alpha smooth muscle actin and vimentin) in both treated and untreated cells. We also used atomic force microscopy to measure the Young modulus of the cells. When treated with TGFβ1, epithelial cells adopted a mesenchymal morphology and displayed indicators of EMT. TGFβ1 stimulated fibroblasts acquired a myofibroblast phenotype, supporting the hypothesis of resident fibroblast activation through TGFβ1 induced FMT.

1 Introduction

1.1 Idiopathic pulmonary fibrosis (IPF)

Lung fibrosis has been extensively studied and classified. Usually, lung fibrosis is induced by traumatic injuries or by toxic or infectious agents, but in some cases (IPF) fibrosis appears without the presence of any obvious external agent [1].

IPF is a form of chronic fibrosing interstitial pneumonia, usually fatal and untreatable, which is found in patients between 50 and 70 years of age at presentation [2]. IPF prevalence ranges from 3-6 cases per 100000 in the UK up to 16-18 cases per 100000 in Finland and depends on location, identifying criteria and year of study [3]. Pathologically, this disease presents unique micro environmental alterations including alveolar epithelial injury, disappearance of the basement membrane, fibroblasts and myofibroblasts over accumulation [4]. This leads to the hardening of the lung tissue, extracellular matrix (ECM) remodeling and increase in several pro-fibrotic soluble factors including transforming growth factor TGF-β [1, 2, 5]. Hystologically, advanced IPF is characterized by the presence of normal lung tissue interspersed with fibroblast foci (areas with a dense population of fibroblasts and myofibroblasts) and areas of honeycombing (their structure is similar to a honeycomb) [2].

IPF exact causes are still to be determined, but the current hypothesis is that it results from epithelial injury and abnormal wound healing.

1.2 Wound healing in the lung tissue

In normal physiological conditions our organism is perfectly capable to repair even severe epithelial injury. When the skin is wounded, the epithelial cells migrate into the injured area, proliferate and differentiate to reconstitute tissue continuity (re-epitelialization). Moreover, the injury of the tissue causes the disruption of the blood flow in order to redo the homeostasis and to create a provisional extracellular matrix. This is where the repair process starts. The deposition of ECM together with fibroblast proliferation, angiogenesis and immune flow generate a granulation tissue rich in small vessels, myofibroblasts, fibroblasts and inflammatory cells. When re-epithelialization is complete, the number of myofibroblasts from the granulation tissue decreases significantly due to apoptosis. Furthermore, the provisional ECM is degraded and the granulation tissue evolves into a scar [6].

In pathological conditions, the adequate re-epithelialization is absent due to a slow epithelial response and the expression of adhesion molecules is altered. During abnormal wound healing, the signals responsible for myofibroblasts apoptosis are absent or delayed. This anomaly helps myofibrob-

lasts to survive and to produce abundant ECM components, which induce impaired re-epitelialization, perpetuated scarring or fibrosis and finally loss of tissue function [2]. In addition, abnormal wound healing is characterized by the hardening of the lung tissue, which is a hallmark of IPF.

1.3 Myofibroblasts in lung fibrosis

Myofibroblasts are activated fibroblasts with smooth-muscle like features. These cells are able to produce proteases that destroy the damaged tissue and are also able to synthesize collagen I required to form the provisional matrix. Moreover, myofibroblasts produce stress fibers rich in α-sma (smooth muscle actin), which contribute to ECM contraction. Due to all these properties, they are very important factors in ECM reorganization and wound contraction [6]. During tissue injury the request for myofibroblasts is believed to be very high and there is evidence suggesting that the myofibroblasts arise from multiple sources. One source is the activation of the resident fibroblasts through fibroblast to myofibroblast transition (FMT) mediated by TGFβ1 [7].

After tissue injury, fibroblasts are activated, migrate to the damaged tissue and start synthesizing ECM. Furthermore, fibroblasts lose their stress-shield provided by ECM in normal tissue and are forced to acquire contractile stress fibers. Tomasek et al. (2002) [6] made a classification of myofibroblasts. They named the ones that only express stress fibers and no α-sma "proto-myofibroblasts" and the ones that express α-sma "differentiated myofibroblasts". When the proto-myofibroblasts are formed (due to mechanical tension), they are stimulated to express α-sma and to turn into differentiated myofibroblasts (Figure 1) [6]. Clinical studies done both in vivo and in vitro showed that TGFβ1 is the key factor in promoting the formation of stress fibers, focal adhesion and fibronectin fibrils, components that characterize the differentiated myofibroblasts. There is also evidence that fibroblasts treated with TGFβ1 express myofibroblast markers and adopt morphological properties of myofibroblasts [8, 10, 9].

Another possible source for myofibroblasts are the epithelial cells. Clinical studies suggested that myofibroblasts arise from epithelial cells as a result of TGFβ1 induced epithelial to mesenchymal transition (EMT) [11, 4]. In order to verify this hypothesis, Willis et al. [11] used one alveolar epithelial cell (AEC) line (AT2) and isolated alveolar epithelial type II cells, which were treated with TGF-β1 for up to 12 days. Using phase imaging and indirect immunofluorescence, Willis et al showed that cells grown with TGFp1 had a fibroblast-like morphology and were expressing a big amount of α-sma fibers compared to the untreated cells. Several studies demonstrate that during kidney, liver and breast fibrosis, TGFβ1 is the key regulator in epithelial cells transdifferentiation [12, 13, 14]. These findings have provided

the motivation to continue the investigations regarding myofibroblasts formation during fibrosis.

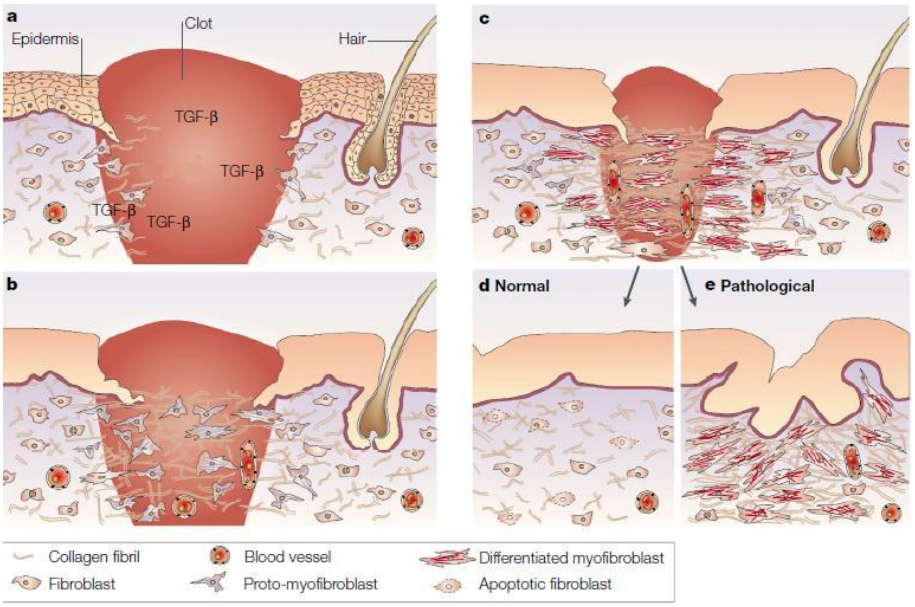

Figure 1: Model of the role of myofibroblasts during the healing of an open wound [6]. a) In normal tissue fibroblasts are stress-shielded by the surrounding ECM. When the tissue is injured, the wound is filled with fibrin and fibroblasts are stimulated by TGFβ1 to invade this provisional matrix. b) Collagen matrix is rearranging due to the forces exerted by migrating fibroblasts. The developing mechanical stress induces stress fibers into fibroblasts, converting them into proto-myofibroblasts. c) Proto-myofibroblasts synthesize alpha smooth muscle actin and evolve into differentiated myofibroblasts, which produce collagen and other ECM components. This continuous loop shortens the collagen matrix and closes the wound. d) In normal conditions, after wound healing, myofibroblasts disappear due to apoptosis. e) In pathologic conditions, myofibroblasts survive and continue producing collagen and remodeling the ECM.

1.4 Epithelial to mesenchymal transition (EMT)

Epithelial cells form monolayers and present apical-basal polarized regularly spaced cell-cell junctions and adhesions between neighboring cells that hold them together. This enables the movement of the whole sheet of cells and prevents individual cells to migrate from the epithelial monolayer. Epithelial cells are characterized by the expression of specific epithelial proteins such as E-cadherin, γ-catenin and cytokeratins. By contrast, mesenchymal

cells have their leading edge polarized front-to-back, do not form uniform structures, are able to move individually due to weak adhesion forces between them and posses resistivity to apoptosis . The proteins expressed in mesenchymal cells are vimentin, fibronectin, α-smooth muscle actin [15].

The transformation of epithelial cells into mesenchymal cells implies changes in morphology, mobility, cellular architecture and adhesion forces, but also induces modifications in phenotypic markers (resistance to apoptotic signals, increased migratory capacity) [15]. During EMT the epithelial units disaggregate and the epithelia changes its shape in order to move. Transition epithelium loses tight and adherens junctions, loses polarity and cytokeratin intermediate filaments. The next step involves F-actin stress fibers rearranging and filopodia and lamelipodia expression. This allows transitioning cells to disrupt basement membranes and to migrate in ECM, a process involved in tumor invasiveness [16].

EMT represents a phenotypic conversion due to molecular reprogramming of epithelium with new biochemical instructions and the result are cells that express both epithelial and mesenchymal markers.

1.5 Aims

The purpose of this thesis was to find what cells are responsible for abnormal tissue hardening: resident fibroblast through FMT or epithelial cells through EMT. In this sense, two different experiments using two different techniques were conducted. In the first experiment epithelial cells and fibroblasts were treated with TGFβ1 and the differences between the mechanical properties (elasticity) of treated and untreated cells were studied using Atomic Force Microscopy (AFM) measurements. This technique is standard and it was successfully applied before for measuring the Young modulus of human alveolar and bronchial cells. In the second experiment immunofluorescence was used in order to check if TGFβ treated cells achieve markers for EMT or FMT.

2 Materials and methods

2.1 Cell culture

The study was performed with human primary lung fibroblasts and lung epithelial cell lines. Epithelial cell lines included: A549, H441 and H1975. A549 were cultured in HEPES (Sigma Chemical, St. Luis, MO) medium, buffered RPMI 1640 with 10% inactivated fetal calf serum (Biological Industries, Kibbutz Beit Haemek, Israel), 100 U/ml penicillin, 1mM L-glutamine, 100 mg/ml streptomycin (GIBCO, Gaithersburg , MD) and 2μg/ml ampho-

tericin B (Bristol-Myers Squibb Co, New Brunswick, NJ). H441 and H1975 were grown in RPMI 1640 with 10% fetal bovine serum (FBS) and 100μM penstreptomycin.

The fibroblasts were provided by the Department of Interstitial Cells, IDIBAPS, Barcelona, Spain. All the cells were incubated into a temperature-controlled chamber at 37 °C in an atmosphere of 5% CO2. 5 days before the measurements, the cells were trypsinated and plated on 3 10-mm diameter glass cover slips, that were previously washed with ethanol and acetone. After plating, the cells were kept 24h in RPMI 1640 medium with 10% FBS and another 24 h in serum free RPMI 1640 medium. For the next 72 h, one cover slip was maintained with RPMI 1640 medium with 0% FBS and a second cover slip was kept with RPMI 1640 medium 0% FBS and treated with TGFβ1.

2.2 Immunostaining

Cells were washed twice with PBS and fixed with formaldehyde for 15 minutes, incubated with a primary antibody (mouse monoclonal anti alpha smooth muscle actin, anti vimentin) diluted in 1% BSA-PBS at 37 °C for 1 hour. After washing 3 times with PBS, the corresponding secondary antibody was added and incubated for 1 hour at 37 °C. Vimentin and alpha smooth muscle actin were stained using secondary antibody conjugated with ALEXA fluor 488 (green). F-actin was stained using falloidin TRITS red. DAPI was used to counterstain the nuclei and incubated for 5 minutes. The samples were mounted with PROLONG GOLD medium and left to dry in the dark.

2.3 Measurements

2.3.1 AFM

The physical properties of the cells were measured with a standalone atomic force apparatus AFM (Bioscope, Veeco) mounted on the stage of an inverted optical microscope (Axiovert S100,Zeiss, Gottingen, Germany). The indentation of the cells was made using silicon nitride triangular cantilevers with nominal spring constant k=0.03 N/m and cantilever length of 20μm (Au coated, Veeco). The cantilever had a regular four-sided pyramidal punch with nominal semiincluded angle Θ=35 degrees. The values of the nominal k and Θ served for data processing.

AFM measurements were carried out at a temperature of 37 °C. The relationship between cantilever's deflection and the photodiode signal was calibrated before cell measurements with the cantilever in contact with a bare region of the cultured glass cover slip. The sensor signals of the recorded

position are in linear relationship with the photodiode. The slope represents the calibration factor. The force F on the cantilever was computed using Hooke's law : F=k*d, where k is the nominal spring constant and d represents the deflection of the cantilever. This deflection was measured with a laser spot focused on cantilever that is reflected off into a photodiode. The elasticity of the cells was probed in the perinuclear region of the cell. For every cell, 3 force-displacement curves (10 $\mu m/s$; 5 μm amplitude) with a maximum force of approximately 4 nN were recorded.

2.3.2 Confocal microscopy

Immunofluorescence images were captured with an inverted microscope system Nikon eclipse Ti series (Nikon Instruments Inc, Melville, NY, USA) using the Metamorph software (Molecular Devices, Downingtown, PA, USA). An automated protocol was developed for image acquisition. A 7 steps routine was developed with the help of the Metamorph software and the motorized stage of the Nikon eclipse Ti microscope in order to automate image acquisition (Figure 2). First, in every sample it was chosen randomly an initial point, which was registered on the stage as coordinate 0. Second, at 7 non-overlapping locations, images were acquired manually using predefined time exposures. The images were exported to Image J (free software from http://rsbweb.nih.gov/ij) as Tiff files.

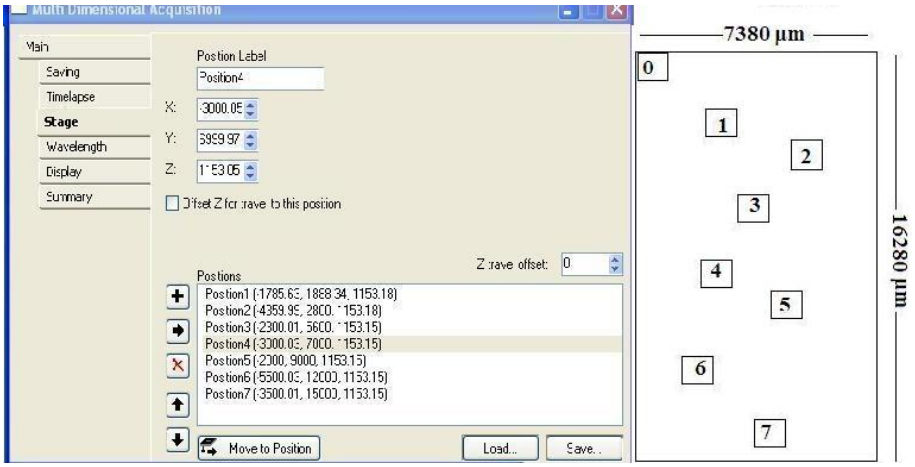

Figure 2: Illustration of the Metamorph routine used to acquire immunofluorescence images. In the left image are presented the coordinates corresponding to each location. In the right image is shown the distribution of the 7 areas within the well. The locations were chosen randomly.

2.4 Data processing

2.4.1 AFM data processing

The correction for the zero-force offset was applied to the force exerted on the cantilever. The force and the indentation of a four-sided pyramidal indenter are related by

$$F = \frac{3Etan\theta}{4(1-\nu^2)}\delta^2 \text{ [17]}$$

E is the Young modulus and ν is Poisson's ratio of the cell. The value of ν was assumed to be 0.5. δ represents the cell indentation depth and it was calculated as δ=z-z_c-d.

In order to compute z_c., Eq. 1 is expressed in terms of z and d

$$z - d = z_c + (\frac{4(1-\nu^2)kd}{3Etan\theta})^{1/2}$$

E and z_c were obtained as least-square fitting parameters of Eq.2 to the loading trace of the F-z curve measured on each cell [17].

2.4.2 Confocal image processing

In order to process the images, two protocols were developed: one was used to calculate the average intensity of a protein (F-actin, alpha smooth muscle actin or vimentin) and another one was used to calculate the fraction of cells that are alpha smooth muscle actin positive within the population (Figure 6).

Average intensity calculation

In order to quantify the level of expression of a given protein, the average intensity of immunofluorescence images (Imean), which was calculated by dividing the total intensity of the image to the total number of pixels in the image (Figure 3), was divided by the total number of nuclei within that image. Moreover, this quantity was averaged for all the seven images acquired in the same well and the result ($I_{average}$) was used to compare the level of expression of a given protein in all the samples.

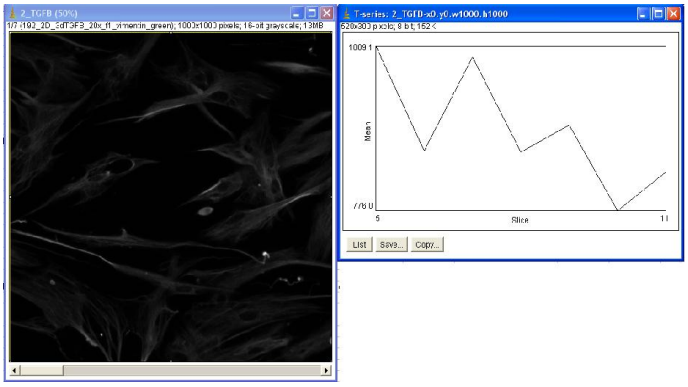

Figure 3: Example of a stack analyzed using the Intensity vs Time plot plugin of ImageJ processing tool. On the left side is showed a representative image acquired in the well treated with TGFβ1 of a sample consisting from fibrotic fibroblasts stained for vimentin. The window in the right is the plot-window that shows the mean intensity corresponding to every image in the stack.

To validate the protocol of Average Intensity Calculation, we measured the expression of vimentin in human lung fibroblasts control and treated with TGFβ1. The cytoskeletal protein was expected not to exhibit any variation and it was used asa negative control. The results are shown in Figure 4.

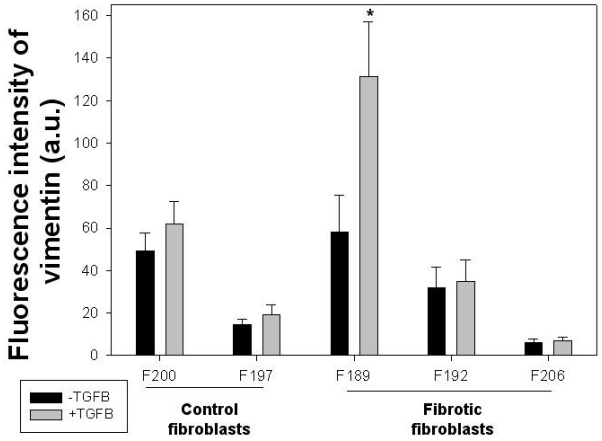

Figure 4: Fluorescence intensity of vimentin measured on human lung normal and fibrotic fibroblasts. Dark bars indicate the control samples (-TGFβ1) and gray bars indicate the treated samples (+TGFβ1). *p<0.05 TGFβ1 treated cells vs control cells.

Quantification of activated cells fraction

The fraction of cells activated with alpha smooth muscle actin was quantified by dividing the number of activated cells from one image (Na) to the total number of cells (Nn) within that image. To find the number of activated cells, the intensity distribution histogram of the alpha smooth muscle actin stained images was analyzed. Depending on the values expressed by the histogram, the same threshold was applied to every image in order to maintain only the pixels with an intensity above a certain threshold value (Figure 5). Images showing the nuclei were merged with alpha-smooth muscle actin images that were processed as described above. Cell counting was done manually by counting nuclei (Figure 6).

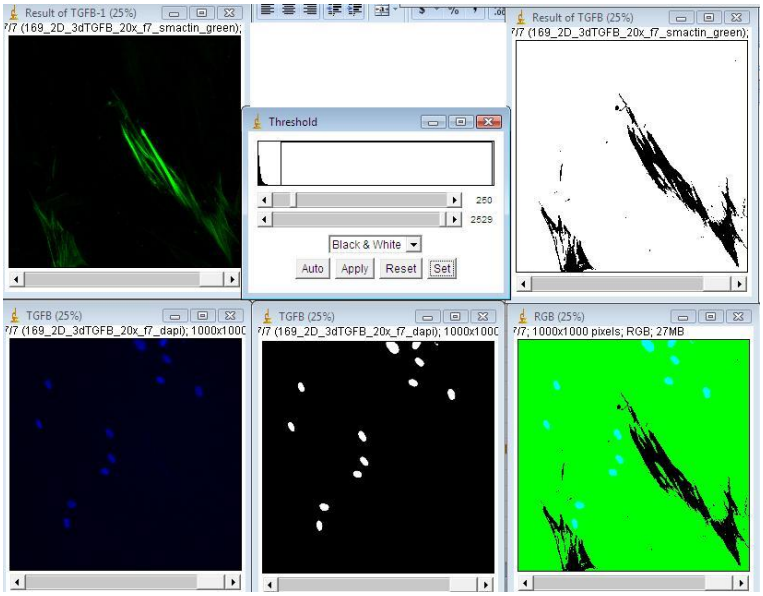

Figure 5: Quantification of the percentage of activated nuclei with alpha smooth muscle actin. The original image showing the expression of alpha-smooth muscle actin was corrected for the background. Next, a threshold for the intensity was applied and the images showing the nuclei and the alpha smooth muscle actin were merged. The result is shown in the bottom right corner.

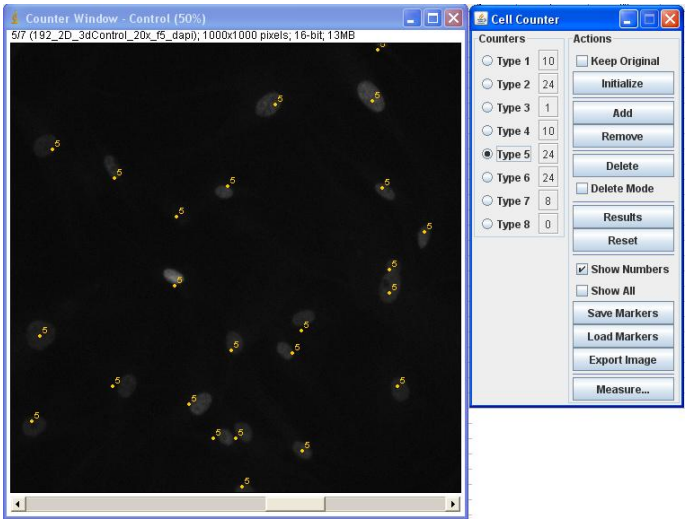

Figure 6: Illustration of the counting process using Cell Counter plugin. Images were acquired in the well containing untreated fibrotic fibroblasts. The image exposed is the fifth in the stack and to analyze it, the Type 5 counter was used. The number of nuclei within this image is saved in the box corresponding to this counter.

2.4.3 Statistical analysis

Significance levels were calculated using Students t-test for unpaired samples. $P<0.05$ was considered significant.

3 Results

TGF β1 induces EMT in human lung epithelial cells

During EMT epithelial cells suffer morphological modifications, gain mobility and start expressing mesenchymal markers such as vimentin. In order to verify if TGFβ1 induces EMT, two human lung epithelial cell lines (A549 and H1975) were activated with TGFβ1 and stained for vimentin. The results are shown in Figure 7. In contrast with the control cells, treated cells expressed significantly more vimentin and presented a wider, spread-out morphology (Figures 8 and 9). Although normal epithelial cells do not express vimentin, A549 and H1975 cells express it even if not treated with TGFβ1, but in a very low amount compared to fibroblasts (data not shown). This is due to their carcinomic origin.

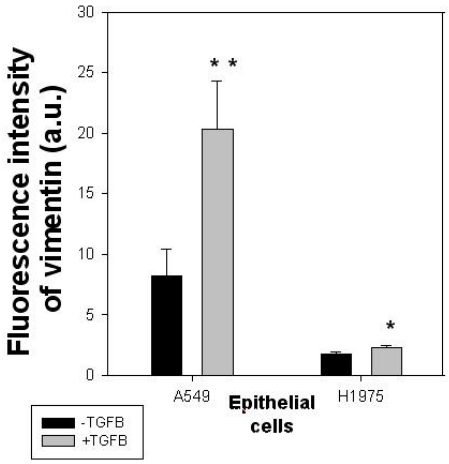

Figure 7: Fluorescence intensity of vimentin measured in control cells (black bars) and TGFβ1 treated cells (gray bars) of A549 and H1975 cell lines. ** $p<0.01$; * $p<0.05$ TGFβ1 treated cells vs control cells.

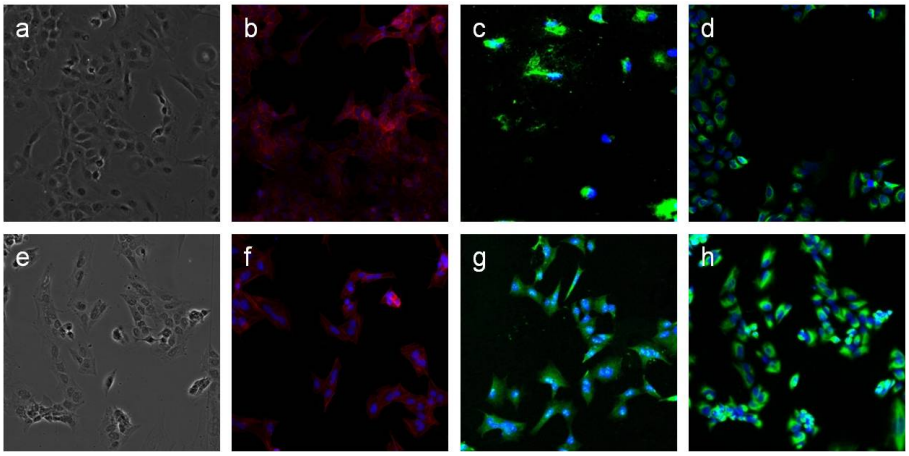

Figure 8: Fluorescence micrographs of A549 cells acquired with an objective of 20x. a-d images were captured in a control (without added growth factor) sample and e-h in a TGFβ1 treated sample. a and e represent phase images of the cells, b and f show the level of F-actin (red), c and g the level of alpha smooth muscle actin (green), d and e the level of vimentin (green). The nuclei are shown in blue.

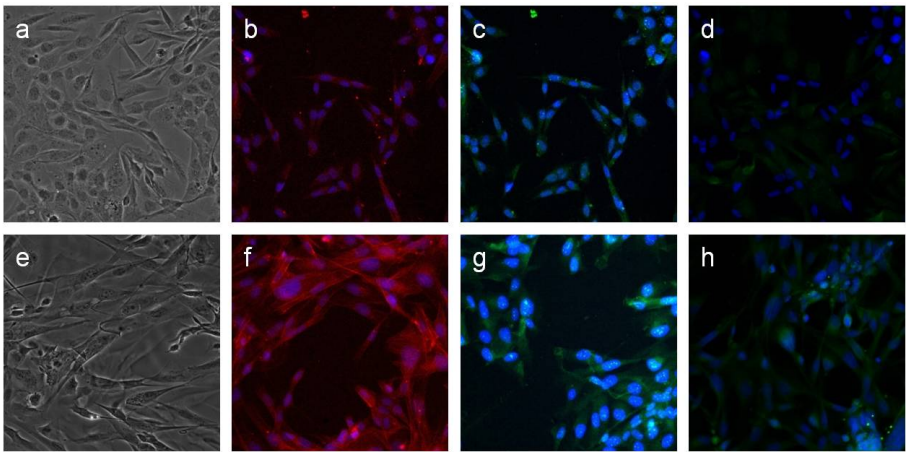

Figure 9: Fluorescence micrographs of H1975 cells. The images were acquired in both control (a-d) and treated (e-h) samples with a 20x objective. a and e represent phase images of the cells, b and f show the level of F-actin (red), c and g the level of alpha smooth muscle actin (green), d and e the level of vimentin (green). The nuclei are shown in blue.

Treatment with TGFβ1 stimulates the increase in alpha smooth muscle actin expression in human lung fibroblasts

Alpha smooth muscle actin is commonly used as a marker for myofibroblast phenotype. We found that control human lung fibroblasts from three different patients suffered a significant increment in the number of cells activated with alpha smooth muscle actin when treated with TGFβ1 (Fgure 10). Moreover, they presented a more fibrogenic appearance compared to the untreated fibroblasts (Figure 11). Fibrotic human lung fibroblasts from three different patients were activated with TGFβ1 and in two cases the number of activated cells with alpha smooth muscle actin was higher than in fibrotic fibroblasts untreated (Figure 10). In the case of human lung epithelial cells, the fraction of activated cells was very low (under 1%) and stimulation with TGFβ1 did not change the number of alpha smooth muscle actin activated cells (Figures 8 and 9, c and g).

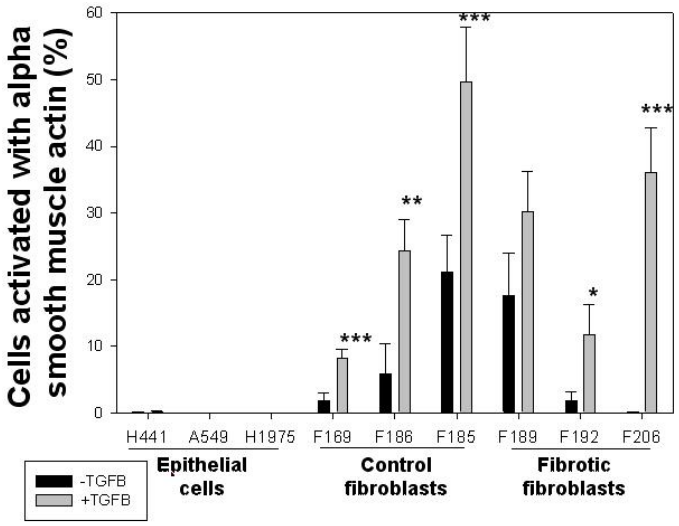

Figure 10: Percentage of cells activated with alpha smooth muscle actin measured in human lung epithelial cells, control fibroblasts and fibrotic fibroblasts. Dark bars show the samples control (-TGFβ1) and gray bars indicate the samples treated with TGFβ1. *** $p<0.005$; ** $p<0.01$; * $p<0.05$ TGFβ1 treated cells vs control cells.

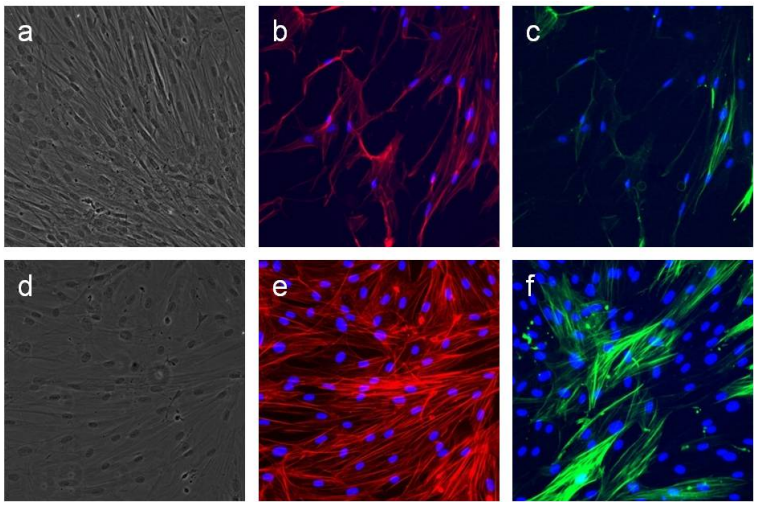

Figure 11: Fluorescence micrographs of healthy human lung fibroblasts (F169). The images were acquired in both control (a-c) and treated (d-f) samples with a 20x objective. a and d represent phase images of the cells, b and e show the level of F-actin (red), c and f the level of alpha smooth muscle actin (green). The nuclei are shown in blue.

Treatment with TGFβ1 leads to an increase in the stiffness of the lung cells

In Figure 12 is showed an example of representative deflection vs z curves recorded in A549 cells. The left curve was measured on a control cell and the right curve was measured on a cell treated with TGFβ1. The behavior of H441 cells and fibroblasts was similar. In the left region of the contact point (indicated by the arrow) the cantilever was not in contact with the cell and the approaching and the withdrawing forces were constant. In the right region of the contact point the force is not linear because the tip is indenting the cell. At low speed (10 μm/s) the hysteresis is caused by the dissipation of the energy within the cell. The slope of the deflection-displacement curve measured in the control cell (left image) is smoother than the slope corresponding to the curve measured in the cell treated with TGFβ1 (right image). This difference is an indicator that the cells become stiffer after being treated with TGFβ1.

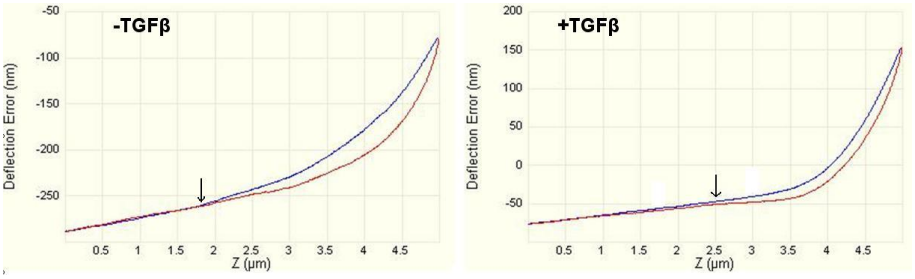

Figure 12: Illustration of the experimental process. The blue and the red lines show the deflection-displacement curve recorded in the perinuclear region of the A549 cells. The deflection-z curves were measured while the piezotranslator was extended (blue line) toward the cell and retracted (red line) at constant velocity (10 μm/s). The hysteresis of the curve is due to the viscoelasticity of the cell. The black arrow indicates the contact point.

The values of the Young modulus measured in both control and TGFβ1 treated cells are shown in Figure 13. It can be seen that in epithelial cells and in fibrotic fibroblasts there is a significant increase in Young modulus values when TGFβ1 is added. In contrast, control fibroblasts do not show differences in stiffness when stimulated with this pro fibrotic factor.

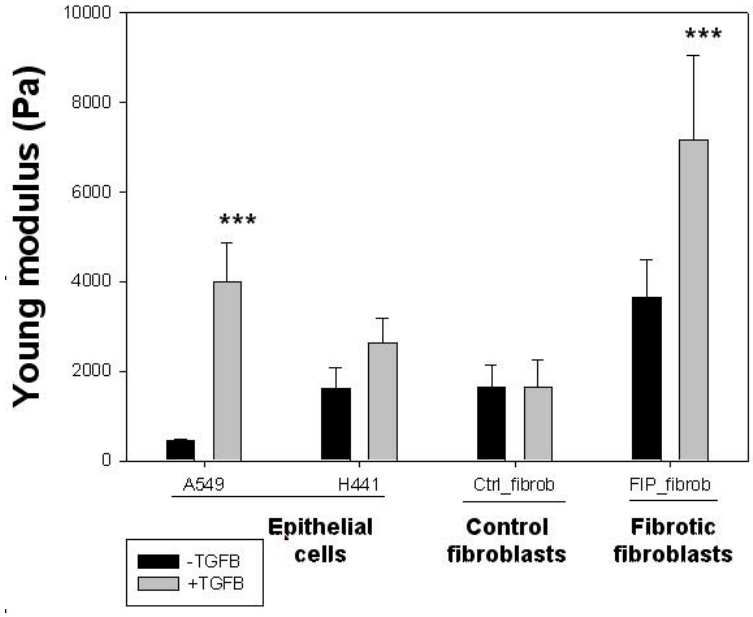

Figure 13: Young modulus measured on control cells (black bars) and TGFβ1 treated cells (gray bars). It is represented the mean value for control and fibrotic fibroblasts. *** $p<0.005$ TGFβ1 treated cells vs control cells.

The influence of TGFβ1 on the expression of F-actin and alpha smooth muscle actin

The level of expression of F-actin augmented significantly in all human lung epithelial cells treated with TGFβ1 (Figure 14). By contrast, the expression of alpha smooth muscle actin did not change in treated epithelial cells (Figure 15, right). Control fibroblasts from two different patients expressed more F-actin when activated with TGFβ1 and the behavior of treated fibrotic fibroblast was similar (Figure 14, right). Although it was noticed an increase in the amount of F-actin in both control and fibrotic fibroblasts stimulated with TGFβ1, in average the difference between control and treated samples was not significant (Figure 14,left). Alpha smooth muscle actin expression was much higher in all activated control fibroblasts and in two samples with treated fibrotic fibroblasts (Figures 15, right, and 16, c and g).

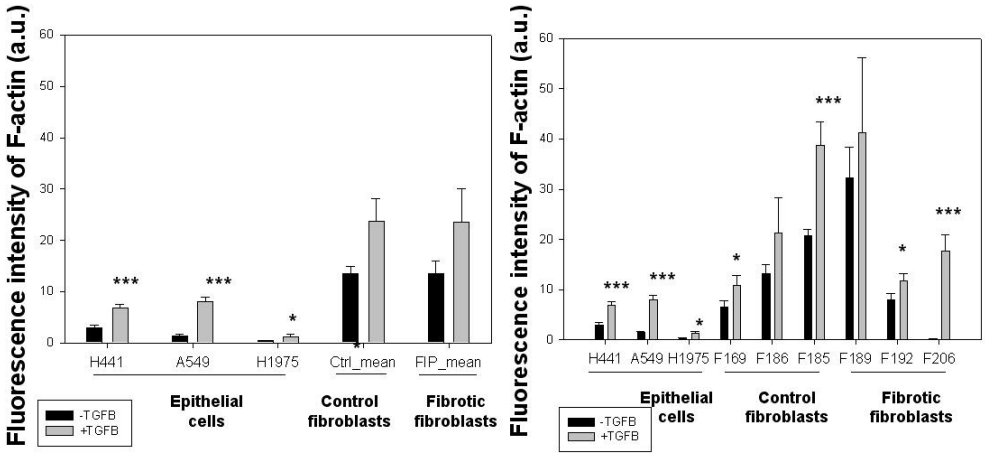

Figure 14: Fluorescence intensity of F-actin measured in normal (black bars) and TGFβ1 treated (gray bars) human lung epithelial cells, control and fibrotic fibroblasts. The image on the left presents the average intensity of F-actin for control and fibrotic fibroblasts. *** p<0.005; ** p<0.01; * p<0.05 TGFβ1 treated cells vs control cells.

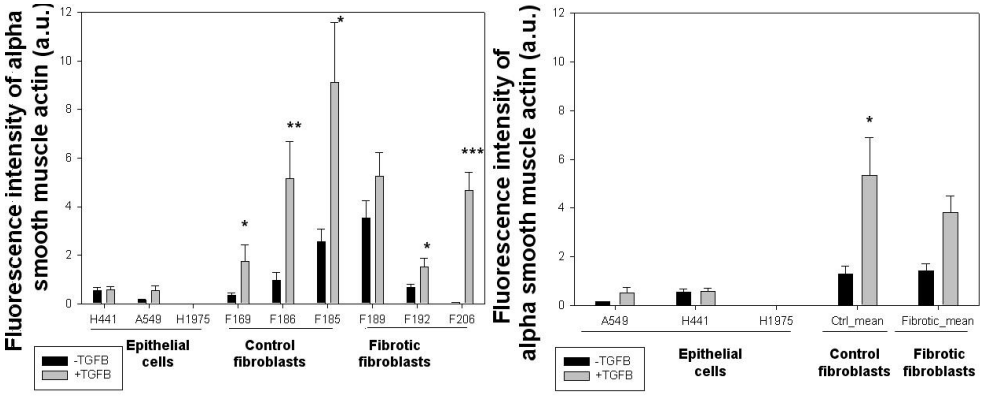

Figure 15: Levels of fluorescence intensity of alpha smooth muscle actin measured in human lung cells. Black bars indicate the control samples and the gray bars indicate the TGFβ1 treated cells. The image on the right shows the averaged values measured in fibroblasts. *** p<0.005; ** p<0.01; * p<0.05 TGFβ1 treated cells vs control cells.

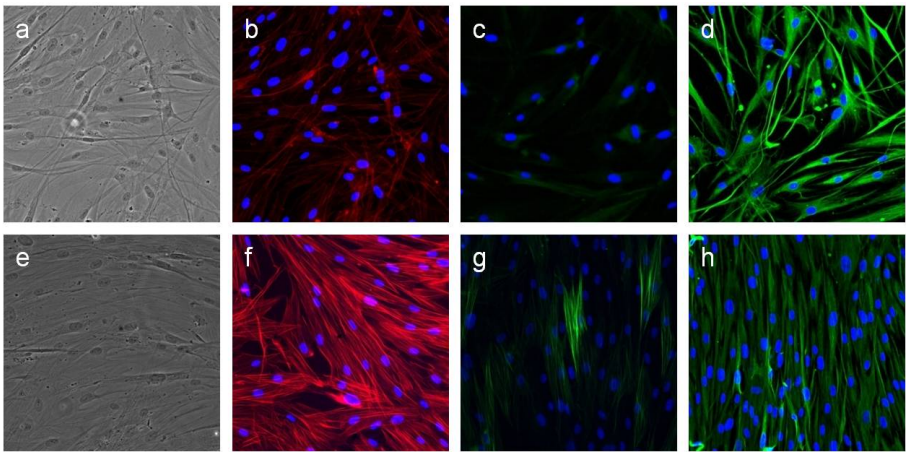

Figure 16: Fluorescence micrographs of fibrotic fibroblasts acquired with an objective of 20x. a-d images were captured in a control sample and e-h in a TGFβ1 treated sample. a and e represent phase images of the cells, b and f show the level of F-actin (red), c and g the level of alpha smooth muscle actin (green), d and e the level of vimentin (green). The nuclei are shown in blue.

4 Discussion

Myofibroblasts are found in granulation tissue [6] and in areas with abnormally high ECM expression [7] during pulmonary fibrosis. These cells are believed to be an important factor during epithelial injury and in promoting ECM deposition, which can lead to tissue hardening and fibrosis. Although their origin is still unknown, myofibroblasts may arise from resident fibroblasts via TGFβ1 induced FMT [6] or from epithelial cells through EMT induced by the presence of TGFβ1 [18, 19].

We treated human lung epithelial cell lines and primary cultured normal and fibrotic fibroblasts with TGFβ1 and we measured the Young modulus (E) in both control and treated cells. E was obtained using the least-squares fitting estimation of the loading F-z curve recorded on each cell. This estimation was used before to characterize the rheology of human epithelial cells [17]. The mechanical behavior of all the untreated cells was similar. By contrast, when stimulated with TGFβ1, cells acted very heterogeneously. While A549 cells and fibrotic fibroblasts exhibit a significant increase in stiffness, H441 and control fibroblasts showed no noticeable difference between treated and untreated cells. This might be correlated with the fact that A549 cells are originated from malignant tissue and fibrotic fibroblasts from fibrotic tissue. At cytological level, epithelial cells stimulated with TGFβ1 showed a very high level of vimentin and F-actin and

adopted a more mesenchymal morphology, all of them indicative of EMT. However, the expression of alpha smooth muscle actin in A549 cells was not significant. This fact in addition to the increase in stiffness suggests that TGFβ1 can induce EMT in human lung epithelial cells, but is not sufficient to transform the epithelial cells into differentiated myofibroblasts.

Differentiated myofibroblasts are commonly characterized by the presence of alpha smooth muscle actin. Previous studies showed that TGFβ1 induces alpha smooth muscle actin expression in rat and human breast fibroblasts [20, 21]. Our results showed that TGFβ1 stimulates the increase in the number of alpha smooth muscle actin activated cells in primary cultured control and fibrotic lung fibroblasts, which supports the hypothesis of TGFβ1 mediated FMT of resident fibroblasts.

Although the increase in stiffness and the high levels of F-actin and vimentin expressed by epithelial cells treated with TGFβ1 could be correlated, this correlation was not observed in normal fibroblasts. While the expression of alpha smooth muscle actin and the number of cells activated with this protein were much higher in treated control fibroblasts than in untreated ones, the level of F-actin and the stiffness were not changing significantly in the presence of TGFβ1. These findings strongly suggest that proteins other than F-actin and alpha smooth muscle actin are involved in the abnormal mechanical responses of control and fibrotic fibroblasts to TGFβ1. Fibrotic fibroblasts exhibited a different behavior after treatment with TGFβ1. They become much stiffer, albeit there was no major increase in the levels of F-actin and alpha smooth muscle actin. This means that stiffness increase is not caused by the apparition of stress and smooth muscle fibers.

Our results were very heterogeneous due to the usage of three different types of cells, with different origins and to one experimental limitations. This limitation was the calculation of the Young modulus for what we assumed that the cell is an incompressible material ($\nu = 0.5$).

5 Conclusions

Atomic force microscopy was used to measure the Young modulus of human lung epithelial cells and primary cultured normal and fibrotic fibroblasts. In normal conditions all the cells revealed similar elastic behavior, but treated with the pro-fibrotic soluble factor TGFβ1 they exhibited a very heterogeneous response. Immunofluorescence was used in order to follow the differences in various cytoskeletal proteins between control and treated cells. By correlating the results, it was seen that TGFβ1 induced morphological and cytoskeletal changes in epithelial cells indicative of EMT, although this was not sufficient to transform the epithelial cells in differentiated myofi-

broblasts. Moreover, TGFβ1 promoted the apparition of F-actin fibers and upregulated smooth muscle actin expression in normal fibroblasts, which is consistent with hypothesis that fibroblast differentiate into myofibroblasts when treated with TGFβ1 (FMT). Activated with TGFβ1 fibrotic fibroblasts become much stiffer, but did not achieve more F-actin or alpha smooth muscle actin, probably because these cells are already transformed.

References

[1] Pardo A., Selman M., Kaminski N.,*Approaching the degradome in idiopathic pulmonary fibrosis*, Int J Biochem Cell Biol **40**: 1141-1155 (2008)

[2] Selman M., King T.E., and Pardo A. *Idiopathic pulmonary fibrosis: prevailing and evolving hypotheses about its pathogenesis and implications for therapy*, Ann Intern Med **134**: 136-151 (2001)

[3] Wilson J.W., du Bois R.M and King T.E. Jr *Challenges in pulmonary fibrosis 8: The need for an international registry for idiopathic pulmonary fibrosis*, Thorax **63** :285-287 (2008)

[4] Kim K.K., Kugler M.C., Wolters P.J., Robillard L., Galvez G.M., Brumwell A.N., Sheppard D., and Chapman H. *Alveolar epithelial cell mesenchymal transition develops in vivo during pulmonary fibrosis and is regulated by the extracellular matrix*, PNAS **103**: 1380-1385 (2006)

[5] Radisky D.C., Kenny P.A., and Bissel M. *Fibrosis and cancer: do myofibroblasts come also from epithelial cells via EMT?*, J Cell Biochem **101**: 830-839 (2007)

[6] Tomasek J., Gabbiani G., Chaponier C., and Brown R.*Myofibroblasts and mechanoregulation of connective tissue remodelling*, Nature **3**: 349-363 (2002)

[7] Hinz B., Phan S.H., Thannickal V.J., Galli A., Bochaton-Piallat M-L., and Gabbiani G. *The myofibroblast. One function, multiple origins*, Am J Pathol **170**: 1807-1816 (2007)

[8] Vaughan M.B., Howard E.W., and Tomasek J.J. *Transforming growth factor-β1 promotes the morphological and functional differentiation of the myofibroblasts*, Exp Cell Res **257**: 180-189 (2000)

[9] Blobe, G.C., Shiemann W.P., Lodish H.F. *Role of transforming growth factor beta in human disease*, N Engl J Med. **342**: 1350-1358 (2000)

[10] Hetzel M., Bachen M., Anders D., Triscler G. and Faehling M. *Different effects of growth factors on proliferation and matrix production of normal and fibrotic human lung fibroblasts*, Lung **183**: 225-237 (2005)

[11] Willis B., Liebler J., Luby-Phelps K., Nicholson A., Crandall E., du Bois R., and Borok Z.*Introduction of epithelial-mesenchymal transition in alveolar cells by transforming growth factor-β1*, AJP **166(5)**: 1321-1332 (2005)

[12] Bachem M.G., Sell K.M., Melchior R., Kropf J., Eller T., and Gressner A.M. *Tumor necrosis factor alpha and transforming growth factor beta stimulate fibronectin synthesis and the transdifferentiation of fat-string cells in the rat liver into myofibroblasts*, Virchows Arch **63**: 123-130 (1993)

[13] Miettinen P.J., Ebner R., Lopez A.R., and Derynck R. *TGF-beta induced transdifferentiation of mammary epithelial cells to mesenchymal cells: involvement of type I receptors*, J Cell Biol. **127**: 2021-2036 (1994)

[14] Fan J-M, Ng Y-Y, Hill P.A., Nikolic-Paterson DJ, Mu W., Atkins R.C., and Lan H.Y. *Transforming growth factor-β regulates tubular epithelial-myofibroblast transdifferentiation in vitro*,Kidney Int **56**: 1455-1467 (1999)

[15] Lee J.M., Dedhar S., Kalluri R., and Thompson E. *The epithelial-mesenchymal transition: new insights in signaling, development, and disease*, J Cell Biol **173**: 973-981 (2006)

[16] Zavadil J. and Bothinger E.P.*TGF-β and epithelial-to-mesenchymal transitions*, Oncogene **24**: 5764-5774 (2005)

[17] Alcaraz J., Buscemi L., Grabulosa M., Trepat X., Fabry B., Farre R., and Navajas D. *Microrheology of human lung epithelial cells measured by atomic force microscopy*, Biophys. J. **84**: 2071-2079 (2003)

[18] Kalluri R. and Neilson E.G. *Epithelial-mesenchymal transition and its implications for fibrosis*, J Clin Invest **112**: 1776-1784 (2003)

[19] Willis BC and Borok Z. *TGF-β-induced EMT: mechanisms and implications for fibrotic lung disease*, Am J Physiol Lung Cell **293**: L525-L534 (2007)

[20] Desmouliere A., Geinoz A., Gabbianni F., and Gabbiani G. *Transforming growth factor-β1 induces α-smooth muscle actin expression in granulation tissue myofibroblasts and in quiescent and growing cultured fibroblasts*, J Cell Biol **122**: 103-111 (1993)

[21] Desmouliere A. *Factors influencing myofibroblast differentiation during wound healing and fibrosis*, Cell Biol Int **19**: 471-476 (1995)